

The role of the mode function in complementarity: A double-slit experiment with entangled photons in different modes

R. Menzel,¹ R. Marx,¹ D. Puhlmann,¹ A. Heuer,¹ and W. P. Schleich^{2,3}

¹*Institut für Physik und Astronomie, Universität Potsdam, D14476 Potsdam, Germany*

²*Institut für Quantenphysik and Center for Integrated Quantum Science and Technology (IQST), Universität Ulm, Albert-Einstein-Allee 11, D-89081 Ulm, Germany*

³*Hagler Institute of Advanced Study at Texas A&M University,*

Texas A&M AgriLife Research, Institute of Quantum Science and Engineering (IQSE), and Department of Physics and Astronomy, Texas A&M University, College Station TX 77843-3572, USA

(Dated:)

We probe the principle of complementarity which is central to quantum mechanics by performing and analyzing a double-slit experiment based on entangled photons created by spontaneous parametric down-conversion due to a pump mode with a coherent double-hump structure (TEM₀₁-mode). In particular, we emphasize the need for a careful selection of the signal-idler photon pairs involved in the corresponding study of visibility and distinguishability. Indeed, when the signal photons interfering at the double slit belong to this double-hump mode we obtain almost perfect visibility of the interference fringes and no which-slit information is available. However, when we break the symmetry between the two maxima of the mode by detecting the entangled idler photon, the paths through the slits become distinguishable and the visibility vanishes. The mode function selected by the detection system decides if interference or which-slit information is accessible in the experiment.

PACS numbers: 42.50.Ar, 42.50.Dv

I. INTRODUCTION

The principle of complementarity [1] of quantum theory [2] can give rise to mind-boggling phenomena [3] in single-photon interference experiments. Examples include, but are not limited to, the quantum eraser [4–6], induced coherence [7?] and delayed-choice experiments [9]. In the present article we report on yet another experiment designed specifically to bring out most clearly these counter-intuitive features and to demonstrate the crucial role of the mode function of light in such investigations.

In a previous experiment [10, 11] we have demonstrated that spontaneous parametric down-conversion (SPDC) can produce astonishing results if the crystal is pumped by a TEM₀₁-mode. For this purpose we have imaged the two intensity humps of the down-converted light onto a double slit in the near field of the crystal as shown in Fig.1. In this way we not only observe the interference pattern in the far field but also obtain which-slit information from the coincidence measurement of the two entangled photons, commonly referred to as signal and idler photon, in the near field. However, in sharp contrast to a naive application of the principle of complementarity we have found a high visibility in the far-field interference pattern of the signal photon even when observed in coincidence with the near-field idler photon.

While our experimental setup is quite elementary and the results could be routinely reproduced the detailed theoretical is demanding because of the complexity of the involved phase matching process. A valuable hint towards an explanation of this surprising phenomenon was given in Ref. [12] arguing that the photons providing us with which-slit information and those which contribute to the interference pattern [13] belong partially to different

photon pairs. This picture is consistent with our earlier observation [10, 11] based on a rather elementary model using a frozen gas of atoms instead of the crystal with its phase matching conditions. Indeed, the atoms creating the entangled photon pair and providing us with which-slit information in the near field are different [3] from those creating the interference in the far field. The principle of complementarity ensures that a single atom cannot yield which-path information *and* interference. More detailed calculations [14, 15] have recently reconfirmed this separation into distinct ensembles of atoms.

Although these arguments demonstrate that the observations reported in Ref. [10, 11] need not to be in contradiction with the principle of complementarity they do not bring out the underlying workings of the experiment. In the present article we fill this gap and show that the phase matching condition [16] for the nonlinear crystal pumped by a TEM₀₁-mode creates different interference patterns in the upper and lower portions of the light cones. Indeed, the upper side reflects the TEM₀₁-mode structure of the single photons at the double slit, while the one at the lower part is of the TEM₀₀-type. This distinction can even be made by the bear eye since the fringes on the top of the ring show a minimum in the middle reflecting the phase shift of π between the two humps of the field at the double slit.

Due to these subtleties in the modes our earlier experiments [10, 11] selected only a small share of the measured photons in agreement with the fair-sampling criticism of Ref. [12, 13]. However, the detailed investigations reported in the present article not only put to rest the remaining questions associated with this discussion but also demonstrate the feasibility of the main idea of [10, 11] to employ the TEM₀₁-pump mode in a test of

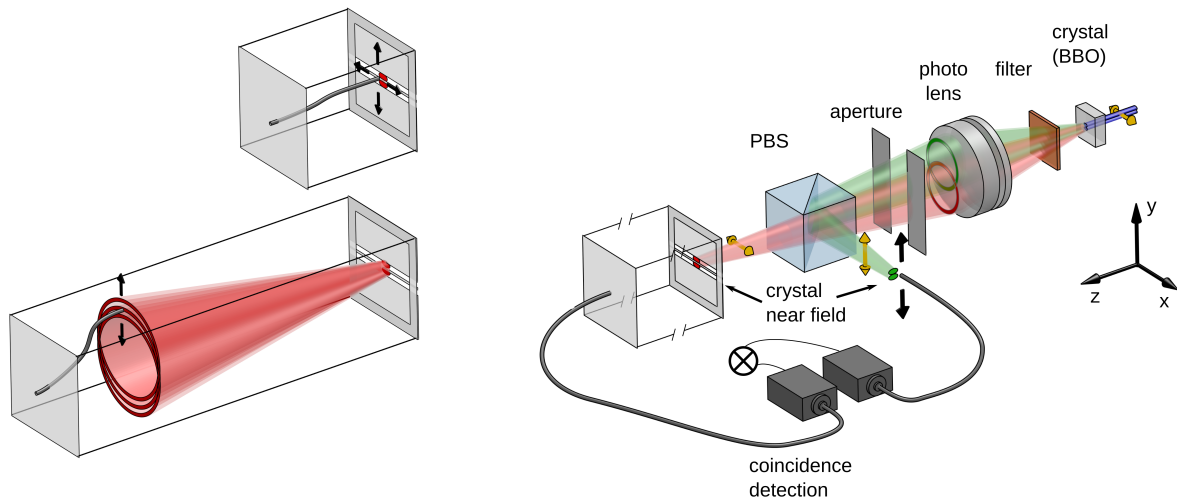


FIG. 1. Which-slit information and interference in a double-slit experiment based on coincidence measurements of entangled photons (right). The photons are created by spontaneous parametric down-conversion (SPDC) due to a light field in a coherent double-hump mode pumping a BBO-crystal [10, 11]. In contrast to our earlier setup we now have apertures in the far-field of the light cones between the photo lens and the polarizing beam splitter (PBS). They select only portions of the emitted bi-photons before obtaining which-slit information (top left) or visibility (bottom left) of the signal photon in the near or far field of the double slit, respectively. Although we here only depict the example of a slit-aperture we also employ circular apertures.

complementarity.

In particular, our analysis confirms that a single photon in a TEM_{01} -like mode structure generated via a thermal SPDC process can produce interference in a double-slit experiment. Photons belonging to the same mode interfere with a high visibility V . However, if the detection system selects photons with increasing which-slit information, that is distinguishability D , they do not belong to the same mode anymore and V decreases. This behavior is the manifestation of complementarity in the spatial domain, demonstrated here for a higher-order Gauss-Laguerre mode. We emphasize that in our experimental arrangement we always satisfy the familiar inequality [17, 18]

$$V^2 + D^2 \leq 1. \quad (1)$$

Our article is organized as follows: In the following section we briefly summarize our double-slit experiment based on entangled photons produced by SPDC with a TEM_{01} -mode and emphasize crucial differences to earlier versions [10, 11] resulting from additional apertures. We then turn in the next section to our experimental observations and explain the asymmetry between the top and the bottom of the light cones formed by the photons. Since our experimental results are in complete agreement with the corresponding numerical simulations [19] we can identify the signal-idler pairs belonging to the same mode. Only these photons have to obey the principle of comple-

mentarity as discussed in the following section. Finally we conclude by summarizing our results.

In order to keep our article self-contained we have included in an appendix (i) an experimental and a numerical study of the influence of a slit-aperture on the visibility and distinguishability, and (ii) an analysis of the phase-matching condition creating the asymmetry in the interference patterns in the light cones.

II. EXPERIMENTAL SETUP: A DOUBLE-SLIT EXPERIMENT WITH ENTANGLED PHOTONS

In this section we briefly describe our experimental setup shown in Fig.1 and discussed in more detail in Ref. [10]. Moreover, we outline our measurement strategy and emphasize differences to our earlier experiments.

The initial TEM_{00} of the pump laser (Toptica, Blue Mode) with a cw-power of 30mW and wavelength of 405nm propagating along the z-axis was converted to a TEM_{01} using a phase plate and the spot size at the crystal was $150 \mu\text{m}$. The BBO-crystal cut for type-II phase matching had [?] a length of 2 mm, and the slits of width $65 \mu\text{m}$ were separated by $235 \mu\text{m}$. The detectors were Perkin Elmer (AQR14) fiber-coupled single-photon avalanche photodiodes.

Since the two light cones formed by the emitted signal and idler photons have different polarizations we can separate them by a polarizing beam splitter (PBS). We

measure the signal photons after a double-slit located in the near field of the crystal which is the imaging plane of its end surface, and aligned parallel to the x-y plane with slits along the x-axis as indicated on the top left of Fig.1.

In another arrangement we use an imaging system to place the signal detector in the far field of the crystal and observe in this way the interference pattern of the signal photons due to the double-slit. Indeed, by moving this detector along the vertical direction as shown in Fig.1 on the bottom left we deduce the visibility

$$V = \frac{R_{max} - R_{min}}{R_{max} + R_{min}} \quad (2)$$

of the interference fringes from the maximal and minimal single photon count rates R_{max} and R_{min} .

The idler detector positioned perpendicular to the signal path behind the beam splitter in the near field of the crystal can also be moved in the vertical direction which corresponds to the detection of the idler photons at the position of the double slit. In this way we obtain which-slit information for the signal photons by taking advantage of their entanglement with the idler photons. The distinguishability

$$D = \frac{C_{S1} - C_{S2}}{C_{S1} + C_{S2}} \quad (3)$$

between the two paths 1 and 2 of the signal photons follows from the coincidence count rates C_{S1} and C_{S2} of the signal photons in path 1 or 2 with respect to the idler photons in path 1.

In contrast to our earlier experiments [10, 11] we now insert between the photo lens and the beam splitter either a slit-aperture as shown in Fig.1, or a circular aperture. These tools allow us to select in the far field of the emitted light cones specific areas of the rings appearing on the detection screen cutting the cones along the x-y plane. In this way we use only a small portion of the ring in the determination of the visibility of the signal photons and restrict ourselves in the which-slit information to those idler photons that belong to the measured signal photons. We shall show that with the help of a circular aperture it is indeed possible to perform for the first time a double-slit experiment with single photons in a TEM_{01} -like-mode structure while simultaneously obtaining which-slit information.

III. RESULTS: DIFFERENT MODES UNRAVELED BY APERTURES

In this section we show that pumping in the TEM_{01} -mode produces a more sophisticated geometrical structure in type-II down-conversion than in type-I which was central to the investigation of Ref. [12]. In particular, it leads to a superposition of modes at the location of

the double slit which has important consequences for the principle of complementarity.

With our crystal of length 2 mm and its optical axis at an angle of 41.9 degree with respect to the y-direction two overlapping rings corresponding to the signal and the idler photons form in the far field. However, these rings are not rotationally symmetric, and this asymmetry is confirmed by our numerical simulations as shown in Ref. [19] and Appendix A.

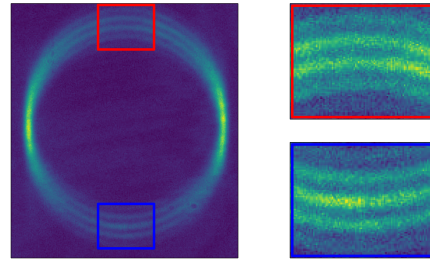


FIG. 2. Asymmetry in the far-field ring pattern (left) of the measured signal photons generated by SPDC using a type-II crystal pumped by a TEM_{01} -mode and having propagated through a double slit. The upper and lower parts show an even (top right) and an odd (bottom right) number of interference fringes, respectively.

Indeed, Fig.2 demonstrates that the light cone of the signal photons in the far-field displays an even and an odd interference pattern on the top and the bottom of the ring, respectively. In order to bring this difference out most clearly we have enlarged these structures in the right column of Fig.2 and emphasize that they are perfectly reproduced in the simulations of Ref. [19].

We study this asymmetry by positioning small apertures in the far field between the crystal and the double slit for the lower and upper parts of the rings. Figure 3 shows that the even substructure in the far field (top left) belongs to the double-hump intensity distribution (middle) at the double-slit position in the near field, and the odd substructure (bottom left) is produced by a non-modulated mode at the double slit (right).

In the latter case we have almost a TEM_{00} -like near-field distribution covering both slits instead of the expected TEM_{01} -mode. Only the upper part with the even interference pattern gives rise to nicely-separated spots reminiscent of the TEM_{01} -mode designed to fit the slit. Indeed, the dip in the middle of the far-field interference pattern behind the slit depicted on the top of Fig.2 is a proof of the phase delay of π between the two humps. As shown in Ref. [10] the photons in this type of mode are in a superposition of two wave vectors giving rise to the familiar far-field interference pattern consisting of two maxima and a zero between them.

Hence, the upper and the lower part of the rings correspond to different modes. In Appendix A we show that they originate from the fact that the phase matching condition in the crystal for a TEM_{01} -pump mode results

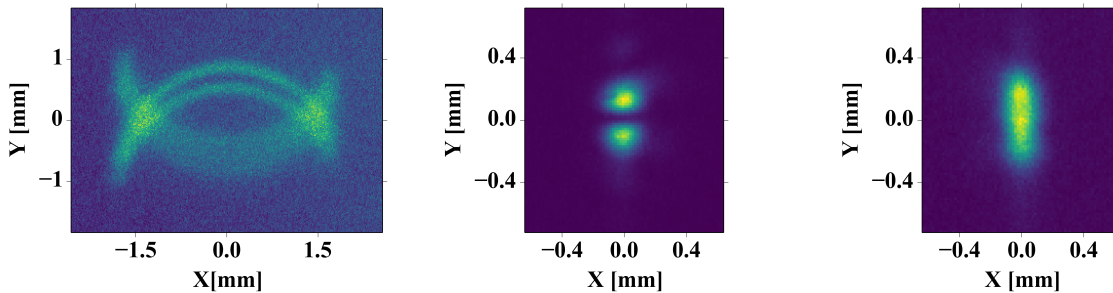


FIG. 3. Superposition of modes unraveled by circular apertures located between the crystal and the polarizing beam splitter (PBS). The upper part of the ring with an *even* number of substructures appearing in the far field (left) belongs to a *double-hump* intensity distribution at the slit (middle), and the *lower part* of the ring with an odd number of substructures (left) is connected to the *non-modulated* distribution at the slit (right). For simplicity both signal and idler photons are measured in the left picture.

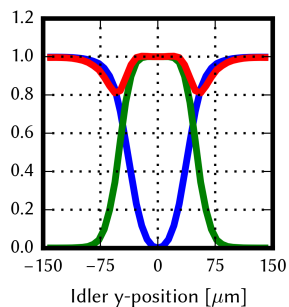


FIG. 4. Verification of the principle of complementarity based on a numerical simulation of our double-slit experiment in the presence of a circular aperture selecting only the double-hump structure at the double slit. Visibility V (green) measured in the far field, and distinguishability D (blue) obtained in the near field of the signal photons behind the double slit in coincidence with the idler photons, together with the sum (red) $V^2 + D^2$ as a function of the transverse position of the idler detector. We emphasize that the red curve never reaches above unity.

in more complex structures of the down-converted light compared to the commonly used TEM_{00} -mode pumping.

IV. DISCUSSION: COMPLEMENTARITY IN ACTION

The deeper understanding of the rather intricate mode structure arising from type-II-phase matching in SPDC pumped by a TEM_{01} -mode gained in the preceding section enables us now to perform a double-slit experiment with the corresponding entangled photons. Since the agreement between simulation and experiment is much better than the experimental error we can base our conclusions on complementarity solely on our theoretical analysis.

In Fig.4 we present a numerical simulation of the visi-

bility V (green), the distinguishability D (blue), and the sum (red) $V^2 + D^2$ in the presence of a circular aperture mapping the TEM_{01} -mode onto the double-slit. Three features stand out most clearly: (i) The which-slit information, that is D , varies when we move the idler detector in near field selecting signal photons across the double-hump structure, from unity to zero, and back to unity. (ii) In this process the visibility V goes from zero to unity, and back to zero, and (iii) we find the equality $V^2 + D^2 = 1$ in the best cases.

The condition for observing high visibility is the non-distinguishability of the photons in the two maxima which occurs when the idler detector is positioned exactly in the middle of the mode. In this case all measured signal photons belong to the TEM_{01} -like mode. When the idler detector is displaced from this position not all measured signal photons belong to this mode anymore. It is these photons which provide us with which-slit information in the near-field correlation measurement.

V. SUMMARY

In summary, we have shown experimentally and by numerical simulations which reproduce all essential features of our experiment that type-II phase matching in SPDC pumped by a TEM_{01} -mode produces a rich variety of light structures dominating single-photon interference and coincidence measurements. The two emitted light cones of the signal and the idler photons are asymmetric. Indeed, the *double-hump* structure of the TEM_{01} -pump mode appears only on the top of the ring. On the bottom we find a *single-hump* TEM_{00} -like intensity distribution. When we investigate the principle of complementarity with bi-photons created in this way we must avoid this mixture of modes by applying circular apertures which select the appropriate photons. They eliminate those that pollute especially the near-field measurement leading to possibly wrong conclusions.

We conclude by emphasizing that the principle of com-

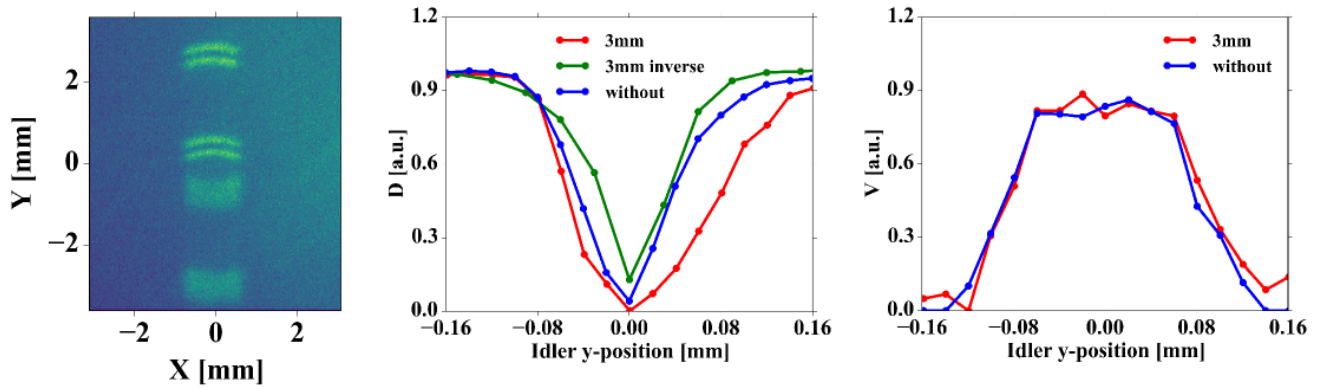


FIG. 5. Influence of a vertical slit-aperture on the visibility V and distinguishability D defined by Eqs. (2) and (3) in the double-slit experiment with entangled photons. Single-photon interference in the far field (left) without the polarizing beam splitter (PBS) but with a vertical aperture between the crystal and the double slit as depicted in Fig.1. The residual upper and lower rings (left) with only 30% of all photons belong to the idler and signal photons. The distinguishability D corresponding to which-slit knowledge (middle) measured in the presence of the PBS for the signal photons behind the double slit as a function of the position of the idler detector depends sensitively on the width of the aperture as illustrated for the three cases of no aperture, one of width 3mm and an inverse aperture (blocking the middle part) of 3mm width. In contrast, the visibility (right) of the signal photons in the far field is almost independent of it.

plementarity in the spatial domain is intimately linked to, and is part and parcel of the detection system. Measuring photons in coherent higher order modes results in high visibility but in no which-slit information, and vice versa.

VI. ACKNOWLEDGMENT

We thank R.W. Boyd, K. Dechoum, B.-G. Englert, L. Happ, M. Hillery, J. Leach, G. Leuchs, P.W. Milonni, M. Efremov, J. Reintjes, M.O. Scully, M.J.A. Sp'ahn, M. Wilkens, M.S. Zubairy, and S.-Y. Zhu for many fruitful discussions on this topic. WPS is grateful to the Hagler Institute for Advanced Study at Texas A&M University for a Faculty Fellowship and to Texas A&M AgriLife Research for the support.

We acknowledge the support of Deutsche Forschungsgemeinschaft (German Research Foundation) and Open Access Publication Fund of Potsdam University.

Appendix A: Apertures and mode matching

In this appendix we summarize experimental results as well as numerical simulations [19] of various aspects of our two-photon double-slit experiment. We first study the effect of the width of the aperture on the visibility V and distinguishability D , and then turn to an explanation of the asymmetry between the top and the bottom parts of the rings created by the light cones of idler and signal photon.

1. Influence of slit-aperture

We start by analyzing V and D as a function of the vertical position of the idler detector in the presence of the slit-aperture indicated in Fig. 1. In this arrangement mainly the middle portions of the rings corresponding to signal and idler photons survive as exemplified by the left part of Fig.A1.

In contrast to the which-slit knowledge D (middle) which sensitively depends on the slit width of the aperture, the visibility V (right) is almost independent of it. The latter result is not surprising because this part of the far field is not influenced by the aperture. The corresponding decrease in D is in agreement with the fair sampling argument of Ref. [12].

Without the aperture a maximum value of $V^2 + D^2 \approx 1.4$ was determined experimentally [12] and theoretically [19] as a consequence of the unfair sampling. However, even in the presence of the vertical aperture violations of the inequality, Eq. (1), occur in specific domains of the position of the idler detector as confirmed by our simulations [19].

Indeed, on the top of Fig.A2 we depict for three different widths of the slit the remaining signal photons. On the bottom we study the corresponding dependence of D , V and the sum $V^2 + D^2$ on the idler position. For a decreasing width the curve (blue) associated with D is broadened, whereas the corresponding one (green) for V is almost unchanged. Only for the narrowest aperture the value (red) of the sum $V^2 + D^2$ is for all positions of the idler detector smaller or equal to unity. Therefore, our simulations confirm the idea [12] of a biased sampling.

2. Asymmetry in the ring

The different interference patterns on the top and bottom of the ring exemplified in Figs. 2 and 3 are a consequence of the details of the phase matching [16] in the type-II crystal pumped by the TEM₀₁-mode. To bring this fact out most clearly we first study the signal photons in the *absence* of the double slit based on a numerical simulation [19]. Figure A3 shows that even then the effect prevails.

In order to understand the influence of this behavior on the coincidence measurements we decompose the bi-photon amplitude distribution

$$\Phi = u(\mathbf{q}_s + \mathbf{q}_i)\xi(\mathbf{q}_s, \mathbf{q}_i) = u(\mathbf{q}_s + \mathbf{q}_i)\text{sinc}(\Delta k_z(\mathbf{q}_s, \mathbf{q}_i)L/2) \quad (\text{A1})$$

into the pump spectral condition and the requirement of phase matching. Here u denotes the transverse mode function of the pump with the wave vectors \mathbf{q}_s and \mathbf{q}_i of the signal and idler photon. Moreover, the type-II crystal of length L leads to a phase miss-match $\Delta k_z(\mathbf{q}_s, \mathbf{q}_i)L/2$.

In the far field the components $q_{s,y}$ and $q_{i,y}$ are linearly related to the spatial coordinates as shown in Fig.A4 by the double-hump structured straight line determined by u . However, the pump condition results in the hyperbolic curve. Only at the intersections of these two qualitatively different curves do we obtain correlated photons.

The signal photon count rates follow from a projection of the coincidence count rate of Fig.A4 onto the corresponding axis. As a consequence, we find in the upper intersection where the two maxima are on top of each other the double-hump intensity distribution shown in the top part of Fig.A5. However, in the lower case where the two spots are next to each other we arrive at a single dominant maximum depicted at the lower part of Fig.A5.

-
- [1] N. Bohr, *Naturwissenschaften* **16**, 245 (1928).
 - [2] D. Bohm, *Quantum Theory* (Dover, New York) (1998).
 - [3] W. P. Schleich *Optics in our Time*, edited by M. D. Alamri, M. M. El Gomati, M. S. Zubairy (Springer, Heidelberg) (2017).
 - [4] M. O. Scully and K. Drühl, *Phys. Rev. A* **25**, 2208 (1982).
 - [5] M. O. Scully, B. G. Englert and H. Walther, *Nature* **351**, 111 (1991).
 - [6] Y. H. Kim, R. Yu, S. P. Kulik, Y. H. Shih and M. O. Scully, *Phys. Rev. Lett.* **84** 1 (2000).
 - [7] X.Y. Zou, L.J. Wang and L. Mandel, *Phys. Rev. Lett.* **67**, 318 (1991).
 - [8] A. Heuer, R. Menzel, and P.W. Milonni, *Phys. Rev. Lett.* **114**, 053601 (2015).
 - [9] X. Ma, J. Kofler and A. Zeilinger *Rev. Mod. Phys.* **88**, 015005 (2016).
 - [10] R. Menzel, D. Puhlmann, A. Heuer and W. P. Schleich, *Proc. Natl. Acad. Sci.* **109**, 9314 (2012).
 - [11] R. Menzel, A. Heuer, D. Puhlmann, K. Dechoum, M. Hillery, M. J. A. Spähn and W. P. Schleich, *J. Mod. Opt.* **60**, 86 (2013).
 - [12] E. Bolduc, J. Leach, F. M. Miatto, G. Leuchs and R. W. Boyd, *Proc. Natl. Acad. Sci.* **111**, 2337 (2014).
 - [13] J. Leach, E. Bolduc, F. M Miatto, K. Piché, G. Leuchs and R. W Boyd *Scientific Reports* **6**, 19944 (2016).
 - [14] L. Happ, Master thesis, Universität Ulm (2015)
 - [15] L. Happ, M. Efremov, K. Dechoum, M. Hillery and W. P. Schleich, to be published (2017)
 - [16] J. F. Reintjes, *Nonlinear Optical Parametric Processes in Liquids and Gases*, (Academic Press, Orlando 1984) .
 - [17] D. M. Greenberger and A. Yasin, *Phys. Lett. A* **128**, 391 (1988).
 - [18] B. G. Englert, *Phys. Rev. Lett.* **77**, 2154 (1996).
 - [19] R. Elsner R, D. Puhlmann, G. Pieplow, A. Heuer and R. Menzel *J. Opt. Soc. Am. B* **32** 1910, (2015).

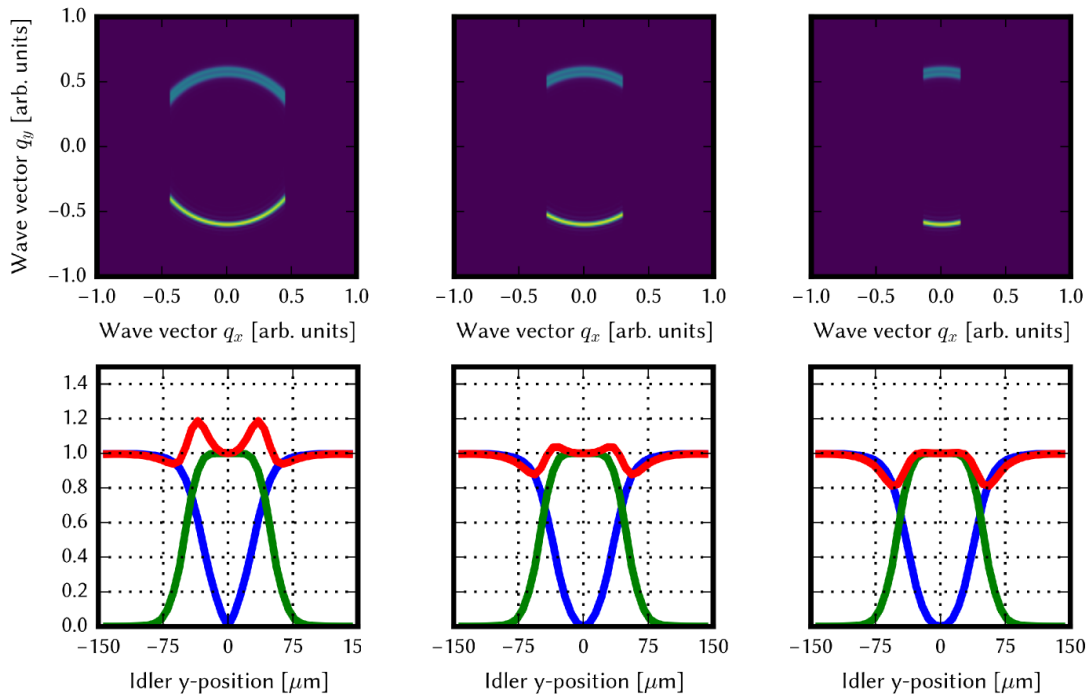


FIG. 6. Influence of the slit width of a vertical aperture on the visibility V (green) and distinguishability D (blue), as well as the sum (red) $V^2 + D^2$ analyzed by a numerical simulation of our experiment. In the top row we depict the signal photons corresponding to 80% (left), 50% (middle) and 23% (right) of the original cone diameter observed in the far-field, that is as a function of the transverse wave vector components q_x and q_y . The remaining signal photons give rise to values of V and D that lead to a violation of the inequality Eq. (1) at *some* positions of the idler detector (bottom left and middle), but also to a situation where this condition is satisfied for *all* locations (bottom right). The scales on the corresponding axis are identical in each row.

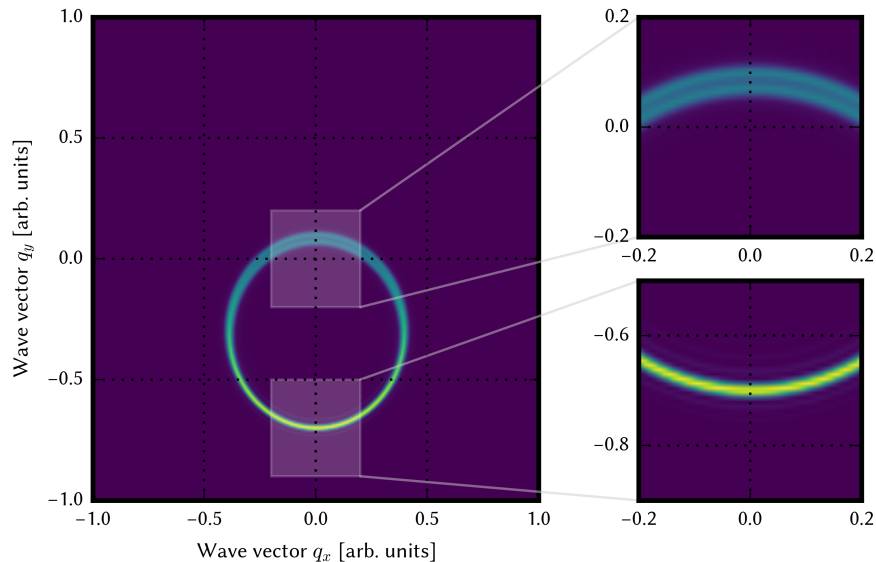


FIG. 7. Asymmetry in the ring obtained by a numerical simulation of the signal photons generated by SPDC using a type-II crystal pumped by a TEM_{01} -mode and observed in the far field without the double slit. Whereas the lower part does not display any modulation the upper one clearly enjoys a double-ring structure.

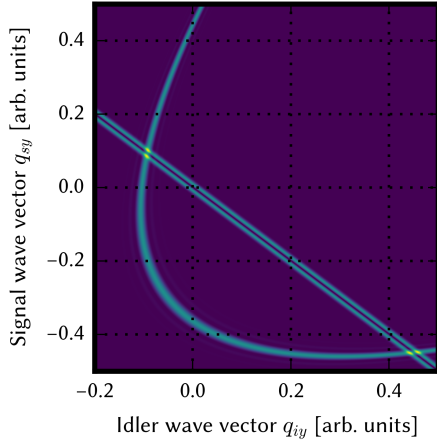


FIG. 8. Origin of the different interference patterns appearing in the top and bottom parts of the ring shown in Fig. A3 identified as energy-momentum conservation required for phase matching. This condition results in transverse wave vector components q_{sy} and q_{iy} which are related to each other in a linear way and depicted here for the two pump humps by straight lines. Energy conservation at the pump and phase matching give rise to a spectral restriction on the two photons which creates the two hyperbolic curves. The two resulting intersections which are qualitatively different – one rather steep and one almost flat – provide us with the emission directions of the two photons.

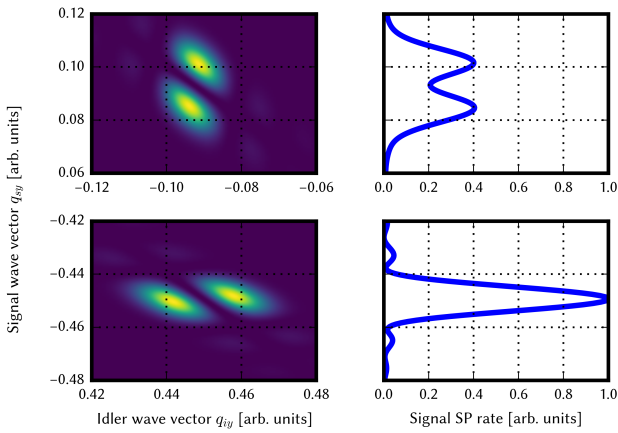


FIG. 9. Signal photon count (SP) rates (right column) as tomographic cuts through the upper (top) and lower (bottom) intersections (left column) of the phase matching curves depicted in Fig. A4. The cuts are along the axis of the wave vector component q_{iy} corresponding to the idler photon.